Ionics (2014) 20:1489–1494
DOI 10.1007/s11581-014-1231-z

SHORT COMMUNICATION

Fabrication of functionalized nitrogen-doped graphene for supercapacitor electrodes

Chunnian Chen · Wei Fan · Ting Ma · Xuwang Fu

Received: 9 July 2014 / Revised: 5 August 2014 / Accepted: 9 August 2014 / Published online: 21 August 2014

Abstract A unique and convenient one-step hydrothermal process for synthesizing functionalized nitrogen-doped graphene (FGN) via ethylenediamine, hydroquinone, and graphene oxide (GO) is described. The graphene sheets of FGN provide a large surface area for hydroquinone molecules to be anchored on, which can greatly enhance the contribution of pseudocapacitance. X-ray photoelectron spectroscopy (XPS), X-ray diffraction (XRD), Raman spectroscopy, and electrochemical workstation are used to characterize the materials. The nitrogen content exhibited in FGN can be up to 9.83 at.%, and the as-produced graphene material shows an impressive specific capacitance of 364.6 F g^{-1} at a scan rate of 10 mV s^{-1}, almost triple that of the graphene (GN)-based one (127.5 F g^{-1}). Furthermore, the FGN electrodes show excellent electrochemical cycle stability with 94.4 % of its initial capacitance retained after 500 charge/discharge cycles at the current density of 3 A g^{-1}.

Keywords Nitrogen-doped graphene · Hydroquinone · Pseudocapacitance · Supercapacitor electrode

Introduction

Supercapacitors have been paid considerable attention recently for their potential applications in areas ranging from electric vehicles to mobile electronic products to satellites, etc., because of the excellent energy storage performance [1–4]. Generally speaking, there are two types of supercapacitors classified on the charge storage mechanism: electrical double-layer capacitor and pesudocapacitor [5–7]. However, during the charge and discharge progress, the pesudocapacitor reveals a lower cycle life and low working voltages than the carbon-based electrical double-layer capacitor [8, 9].

Graphene, as a 2D carbon nanostructure, has shown great potential as a supercapacitor, mainly because of its large theoretical specific surface area (≈2,630 m^2 g^{-1}), high conductivity, and chemical stability [10, 11]. Hence, graphene is widely used in electrochemical supercapacitor fields [12–19]. Recently, nitrogen-doped graphene (GN) has been paid great attention because nitrogen doping can improve the properties of graphene. For example, nitrogen doping can change the chemically derived functionalized graphene from being a p-type to an n-type semiconductor [20, 21]. Moreover, by using N doping, the electron transfer efficiency of graphene can be enhanced [22]. Constitutionally, the GN-based materials are acting as double-layer capacitors [23].

However, it is rare to find researches on attaching quinoid/hydroquinone structure organic molecules onto the GN sheets which can add pseudocapacitance effectively. Herein, we first report a unique and convenient one-step hydrothermal process for synthesizing functionalized nitrogen-doped graphene (FGN) for storing energy as a supercapacitor electrode using ethylenediamine, hydroquinone, and graphene oxide (GO). The reaction mechanism sketch of the FGN is shown in Scheme 1. During the hydrothermal reaction, ethylenediamine molecules continually react with the oxygen functional groups of GO. Ethylenediamine acts not only as a reducing agent to remove the oxygen functional groups of GO but also as a nitrogen source to realize the nitrogen doping. Simultaneously, hydroquinone molecules are adsorbed on the surface of graphene sheets by π-π interaction, which has also been observed in similar systems of graphene with π-conjugated molecules [24–26]. Graphene sheets of FGN provide a large surface area for hydroquinone molecules to attach on, which can greatly enhance the contribution of pseudocapacitance.

C. Chen (✉) · W. Fan · T. Ma · X. Fu
Anhui Key Laboratory of Controllable Chemistry Reaction & Material Chemical Engineering, Hefei University of Technology, Hefei 230009, Anhui, People's Republic of China
e-mail: chencn@hfut.edu.cn

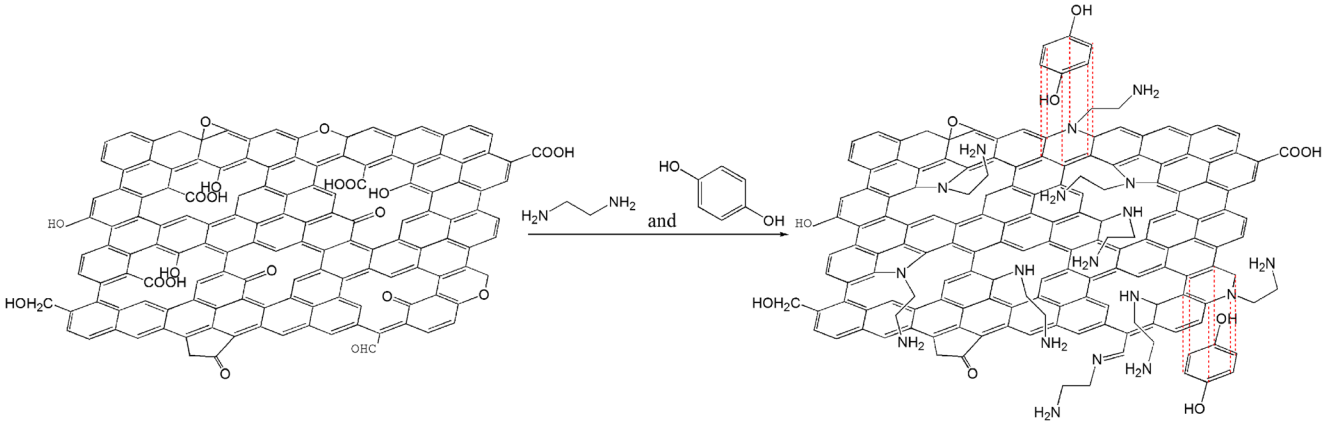

Scheme 1 Reaction mechanism sketch of the FGN

Moreover, the interconnected porous structure of FGN can facilitate hydronium ion diffusion into the pores as well as electron transport throughout the entire graphene framework.

Experiments

GO preparation

GO aqueous dispersion was prepared by oxidation and exfoliation of natural graphite under acidic conditions by a modified Hummers method [27].

Synthesis of GN

Fifty microliters of ethylenediamine and 30 mL of GO (1 mg/mL) suspensions were mixed in a flask and ultrasonically stirred for 0.5 h, then transferred into an autoclave with a volume of 50 mL. Hydrothermal treatment of this mixed solution was at 180 °C for 12 h. After the autoclave naturally cooled to room temperature, the as-prepared black product was then washed with deionized water three times in order to remove residual unreacted compounds. Finally, the sample was vacuum dried for further characterization.

Synthesis of FGN

Fifty microliters of ethylenediamine, 300 mg of hydroquinone, and 30 mL of GO (1 mg/mL) suspensions were mixed in a flask and ultrasonically stirred for 0.5 h, then transferred into an autoclave with a volume of 50 mL. Hydrothermal treatment of this mixed solution was at 180 °C for 12 h. After the autoclave naturally cooled to room temperature, the as-prepared black product was then washed with deionized water three times in order to remove residual unreacted compounds. Finally, the sample was vacuum dried for further characterization.

Electrochemical characterization

All the electrochemical tests were carried out in a standard three-electrode cell with a platinum foil as the counter electrode and a saturated calomel reference electrode and using an aqueous H_2SO_4 solution (1 M) as electrolyte.

The working electrodes were prepared using desiccative materials mixed with acetylene black and polyvinylidene fluoride at a mass ratio of 80:10:10 then dissolved in *N*-methyl pyrrolidone to form a slurry. Next, the slurry was evenly coated onto a gauze platinum electrode. Finally, the working electrodes were placed into a vacuum drying oven at 40 °C for 12 h.

Results and discussion

Morphology of the composite

The field emission scanning electron microscopy (FESEM) image reveals that the vacuum-dried FGN has an interconnected mesoporous network with submicrometer and micrometer pores. The pore walls consist of the thin layers of stacked graphene sheets with some corrugation and scrolling (Fig. 1). The interconnected porous structure can facilitate hydronium ion diffusion into the pores as well as electron transport throughout the entire frame working electrode.

XRD analysis

The structures of GN and FGN were further characterized by X-ray diffraction (XRD). As revealed by Fig. 2a, the broad peaks indicate the poor ordering of graphene sheets which are composed of a few layers stacked. The XRD pattern of GN exhibits a broad peak centered at $2\theta=24.47°$, corresponding to the graphitic (002) profile with an interlayer spacing of 0.363 nm. However, the interlayer spacing of FGN is

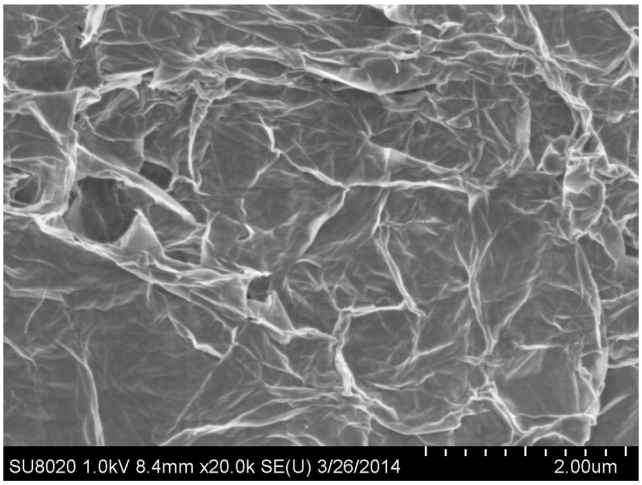

Fig. 1 SEM image of the typical FGN microstructures

0.339 nm which is slightly smaller than that of GN, indicating the existence of π-π stacking between graphene sheets and hydroquinone molecules in FGN.

XPS analysis

X-ray photoelectron spectroscopy (XPS) is a significant method to research the composition of each element as well as functional groups in FGN. As shown in Fig. 2b, the nitrogen content exhibited in FGN can be up to 9.83 at.%, which is a bit higher than the previous reports [28]. The specific content of nitrogen is shown in Fig. 2c. The peak at 398.7 eV is ascribed to pyridinic N, and the peak at 399.3 eV can be attributed to amine moieties. The peak at 400.1 eV can be ascribed to the pyrrolic structure, and the peak at 401.1 eV corresponds to graphitic N or protonated N [29–31]. It means that the nitrogen element is doped into the sheets of graphene successfully. Researchers have demonstrated nitrogen-doped active sites (pyridinic N especially) on graphene sheets that can provide reaction sites for electrochemical reactions [32, 33]. These active sites have a great effect on promoting the oxidation-reduction reaction of hydroquinone molecules which are adsorbed on the surface of the graphene sheet. Similarly, from the high resolution of the C1s spectrum of FGN (Fig. 2d), four

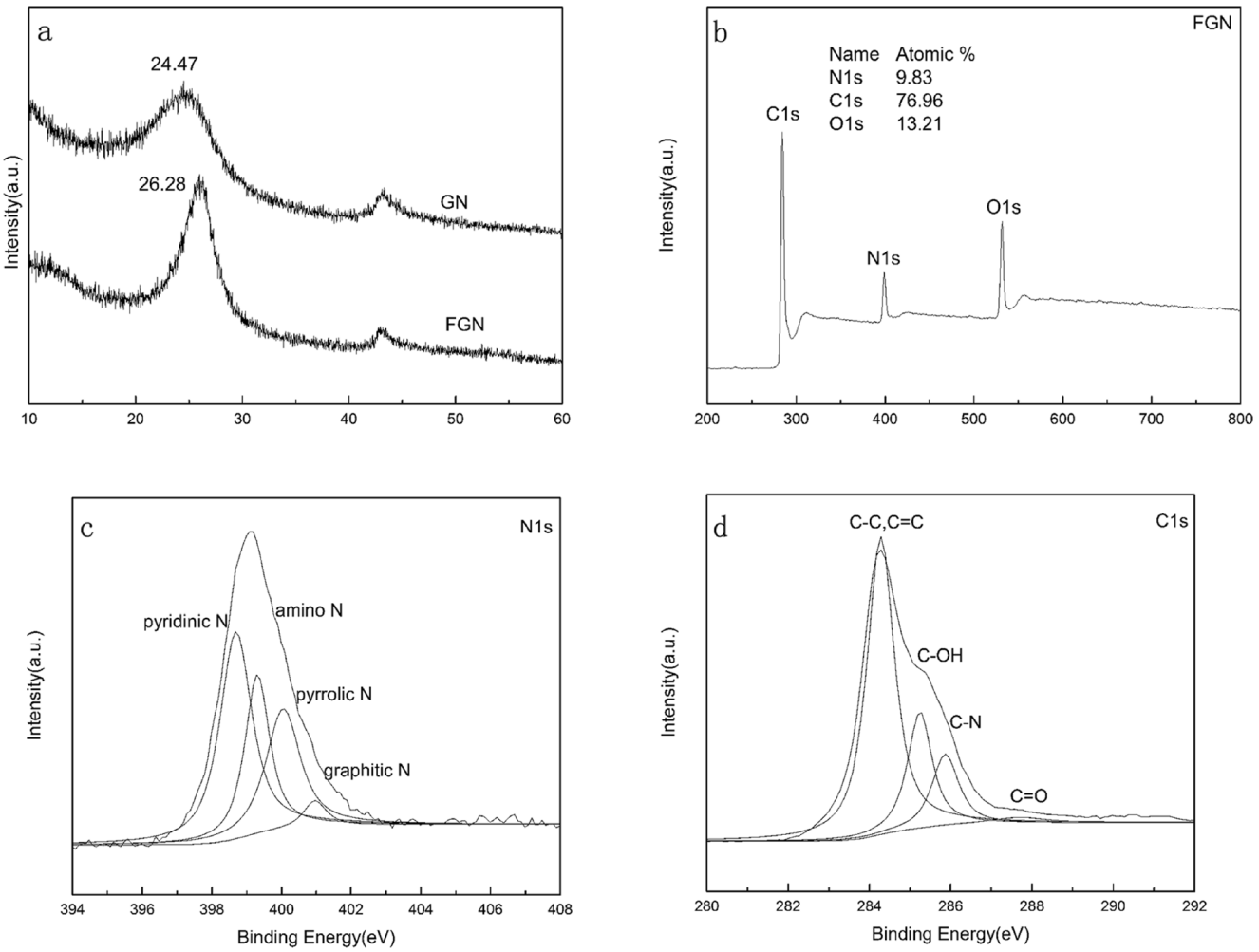

Fig. 2 **a** XRD patterns of GN and FGN. XPS spectra of FGN: **b** wide scan spectra, **c** N1s spectra, **d** C1s spectra

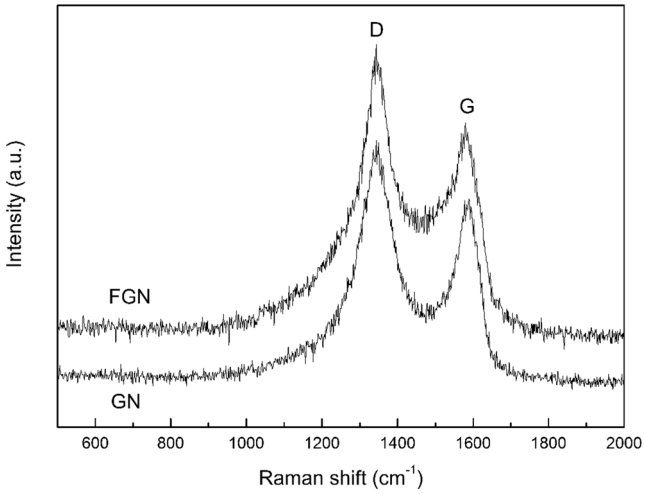

Fig. 3 Raman spectra of FGN and GN

main peaks can be seen. The peak at 284.3 eV corresponds to the sp^2-hybridized graphitic carbon, and the peaks at 285.2, 285.9, and 287.8 eV are attributed to the C–OH, C–N, and C=O functional groups, respectively [34].

Raman spectra analysis

Raman spectroscopy is another very useful technique to characterize carbonaceous materials. Figure 3 shows the Raman spectra of GN and FGN at an excitation wavelength of 532 nm. The peak at 1,344 cm^{-1} attributes to the D band which is associated with structural defects and partially disordered structures of the sp^2 domains [35]. It clearly shows that the intensity ratio I_D/I_G of FGN is 1.35, but the ratio of GN is 1.30. The value was increased due to the hydroquinone molecules anchored on the graphene basal plane. The peak around 1,580 cm^{-1} is called G band related to the E_{2g} vibration mode of sp^2 carbon domains which usually are used to explain the degree of graphitization [30, 35]. Compared with the peak of GN, a blueshift of the G band can be found in FGN, almost 8 cm^{-1}. This is mainly because the hydroquinone molecules

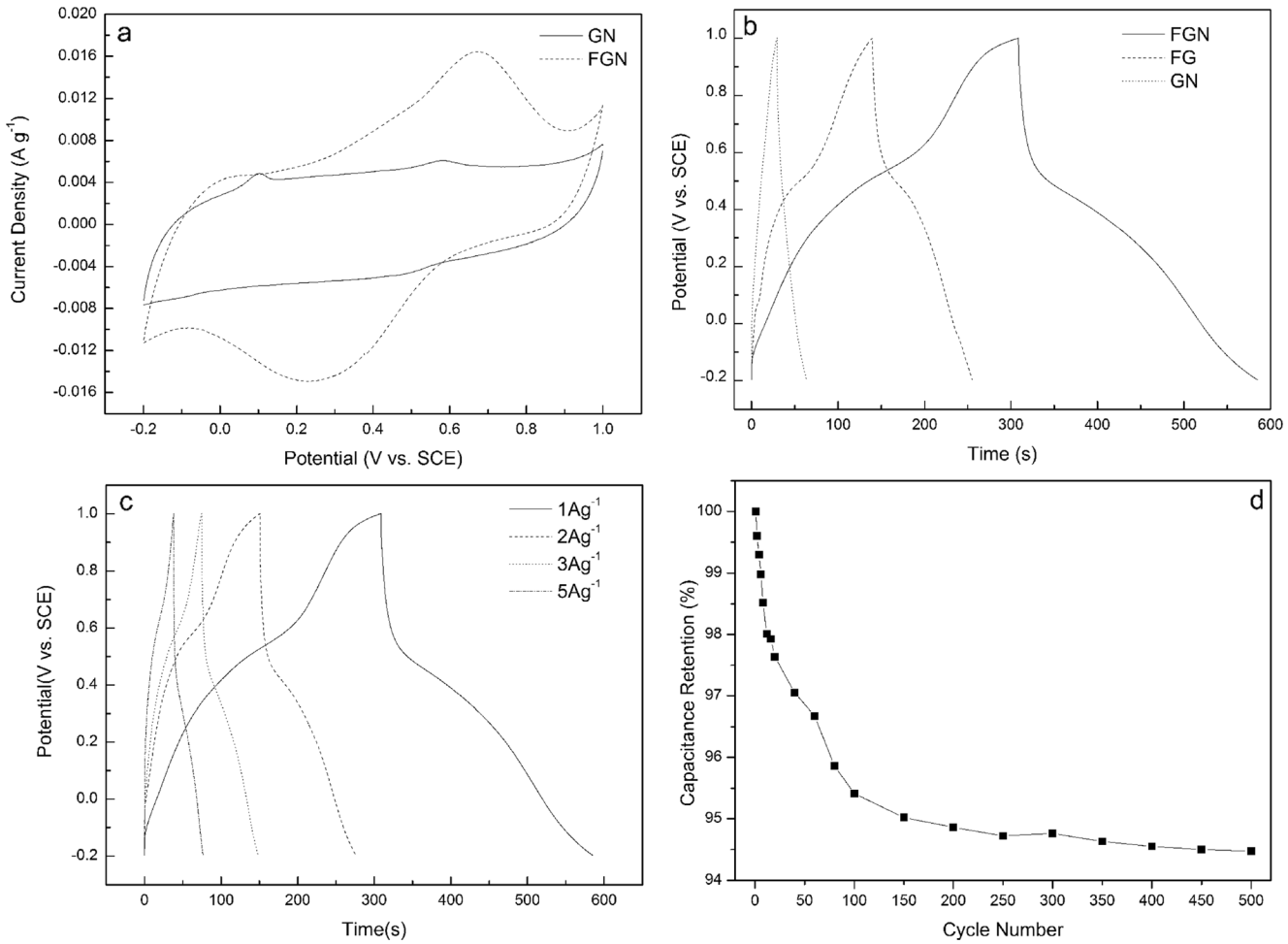

Fig. 4 **a** Comparison of CV curves of GN and FGN at a scan rate of 10 mV s^{-1}. **b** Comparison of galvanostatic charge/discharge curve of FGN, FG, and GN at the current density of 1 A g^{-1}. **c** Galvanostatic charge/discharge curve of FGN at the current density of 1, 2, 3, and 5 A g^{-1}, respectively. **d** Cycling stability of FGN at the current density of 1 A g^{-1}

are adsorbed on the surface of graphene sheets by π-π interactions, and it leads to the variation of charge density in graphene.

Electrochemical performance

Figure 4a shows the cyclic voltammetry (CV) curves of the FGN-based and GN-based supercapacitors. It can be seen that the CV curve of GN exhibits a willow leaf shape, implying pure electrical double-layer capacitive behavior. In contrast, the CV curve of FGN displays a pair of remarkable peaks, which corresponds to the redox reaction of the adsorbed hydroquinone molecules (hydroquinone↔quinone+$2H^+$+$2e^-$) and indicates the coexistence of both the electrical double-layer capacitance and pseudocapacitance. The FGN-based supercapacitor shows an impressive specific capacitance of 364.6 F g^{-1} at a scan rate of 10 mV s^{-1}, almost triple that of the GN-based one (127.5 F g^{-1}).

The galvanostatic charge/discharge curve of FGN shows a deviation from the ideal triangle shape exhibited by GN (Fig. 4b). This result also confirms the inspiring contribution of pseudocapacitance. Moreover, we can obviously find that the FGN-based material has a larger capacitance when comparing the charge/discharge curve of FGN with that of FG (without adding any nitrogen source during the reaction progress). Because by using N doping, the redox reactions between the electrolyte ions and hydroquinone molecules as well as the surface wettability, and electronic conductivity have been improved. [36, 37]. The special capacitances are 243.8, 230.3, 185.3, and 159.4 F g^{-1} at a current density of 1, 2, 3, and 5 A g^{-1}, respectively (Fig. 4c). A long cycle life is another important concern for practical application of supercapacitors containing pseudocapacitance. Importantly, the FGN electrodes show excellent electrochemical stability with 94.4 % of its initial capacitance retained after 500 charge/discharge cycles at the current density of 3 A g^{-1} (Fig. 4d). The marvelous stability indicates that the non-covalent interactions between hydroquinone and graphene are strong enough to sustain a long cycle life.

Conclusion

In summary, functionalized nitrogen-doped graphene was successfully synthesized via a convenient one-step hydrothermal process. The unique nanostructures of graphene sheets provide huge areas for pseudocapacitive hydroquinone molecules to attach on effectively. Meanwhile, doping nitrogen offers abundant electrochemically active functional groups on the graphene sheets. Besides, the interconnected meso- and macro-porous structure of FGN can facilitate ion diffusion throughout the entire porous network. Results show that the FGN reveals outstanding electrochemical performance as an electrode for supercapacitors in terms of specific capacitance (364.6 F g^{-1} at a scan rate of 10 mV s^{-1} and 243.8 F g^{-1} at a current density of 1 A g^{-1}) and excellent electrochemical stability with 94.4 % of its initial capacitance retained after 500 charge/discharge cycles at the current density of 3 A g^{-1}.

Acknowledgments The authors gratefully acknowledge financial support from the Hefei University of Technology, school-enterprise cooperation projects production (106–433168) of China.

References

1. Brownson DAC, Kampouris DK, Banks CE (2011) J Power Sources 196:4873
2. Sheng KX, Sun YQ, Li C, Yuan WJ, Shi GQ (2012) Sci Rep 2:247
3. Frackowiak E, Beguin F (2001) Carbon 39:937
4. Gao B, Hao L, Fu QB, Su LH, Yuan CZ, Zhang XG (2010) Electrochim Acta 55:3681
5. Ramya R, Sangaranarayanan MV (2008) J Chem Sci 120:25
6. Paul S, Lee YS, Choi JA, Kang YC, Kim DW (2010) Bull Chem Soc 31
7. Li J, Xie HQ, Li Y (2013) J Power Sources 241:388
8. Sun YQ, Wu QO, Shi GQ (2011) Energy Environ Sci 4:1113
9. Liu R, Lee SB, Am J (2008) Chem Soc 130:2942
10. Huang Y, Liang JJ, Chen YS (2012) Small 8:1805
11. Zhai YP, Dou YQ, Zhao DY, Fulvio PF, Mayes RT, Dai S (2011) Adv Mater 23:4828
12. Kuila T, Mishra AK, Khanra P, Kim NH, Lee JH (2013) Nanoscale 5: 52
13. Wang DW, Min YG, Yu YH, Peng B (2014) J Colloid Interface Sci 417:270
14. Stoller MD, Ruoff RS (2010) Energy Environ Sci 3:1294
15. Lee JH, Park N, Kim BG, Jung DS, Im K, Hur J, Choi JW (2013) ASC Nano 10(7):9366
16. Wang XB, Zhang YJ, Zhi CY, Wang X, Tang DM et al (2013) NAT COMMUN 4:2905
17. Cui CJ, Qian WZ, Yu YT, Kong CY, Yu B, Xiang L, Wei F (2014) J Am Chem Soc 136:2256
18. Wen ZH, Wang XC, Mao S, Bo Z, Kim HJ, Cui SM et al (2012) Adv Mater 24:5610
19. Chen W, Rakhi RB, Alshareef HN (2013) Nanoscale 5:4134
20. Li XL, Wang XR, Zhang L, Lee SW, Dai H (2008) J Mar Sci 319: 1229
21. Wang XR, Li XL, Zhang L, Yoon Y, Weber PK, Wang HL, Guo J, Dai H (2009) J Mar Sci 324:768
22. Wei DC, Liu YQ, Wang Y, Zhang H, Huang L, Yu G (2009) Nano Lett 9(5):1752
23. Jeong HM, Lee JW, Shin WH, Choi YJ, Shin HJ, Kang JK, Choi JW (2011) Nano Lett 11:2472
24. Xu YX, Lin ZY, Huang XQ, Wang Y, Huang Y, Duan XF (2013) Adv Mater 25:5779
25. Wuest JD, Rochefort A (2010) Chem Commun 46:2923
26. Xue T, Jiang S, Qu YQ, Su Q, Chen R, Dubin S, Chiu CY, Kaner R, Huang Y, Duan XF (2012) Angew Chem Int Ed 51:3822
27. Hummers WS, Offeman REJ (1958) Am Chem Soc 80:1339–9
28. Wang HB, Maiyalagan T, Wang X (2012) ACS Catal 2:781
29. Chen P, Yang JJ, Li SS, Wang Z, Xiao TY, Qian YH, Yu SH (2013) Nano Energy 2:249

30. Sheng ZH, Shao L, Chen JJ, Bao WJ, Wang FB, Xia X (2011) H ASC Nano 5(6):4350
31. Wang DW, Min YG, Yu YH, Peng B (2014) J Colloid Interface Sci 417:270
32. Qu LT, Liu Y, Baek JB, Dai LM (2010) ASC Nano 4:1321
33. Guo HL, Peng S, Xu JH, Zhao YQ, Kang XF (2014) Sensors Actuators B Chem 193:623
34. Singh D, Joung D, Zhai L, Das S, Khondaker S, Seal S (2011) Prog Mater Sci 56:1178
35. Kudin KN, Ozbas B, Schniepp HC, Prud'homme RK, Aksay IA (2008) Nano Lett 8:36
36. Wang HB, Maiyalagan T, Wang X (2012) ASC Catal 2:781
37. Han J, Zhang LL, Lee S, Oh J, Lee KS, Potts JR, Ji JY, Zhao X, Ruoff RS, Park S (2013) ASC Nano 7:19